Journal of Catalysis 261 (2009) 9–16

Contents lists available at ScienceDirect

Journal of Catalysis

www.elsevier.com/locate/jcat

Fe-promotion of supported Rh catalysts for direct conversion of syngas to ethanol

Mohammad A. Haider, Makarand R. Gogate, Robert J. Davis *

Department of Chemical Engineering, University of Virginia, 102 Engineers' Way, P.O. box 400741, Charlottesville, VA 22904-4741, USA

ARTICLE INFO

Article history:
Received 1 September 2008
Revised 16 October 2008
Accepted 18 October 2008
Available online 13 November 2008

Keywords:
CO hydrogenation
Ethanol
Acetaldehyde
Rh/TiO_2 catalyst
$Rh–Fe/TiO_2$ catalyst
FTIR spectroscopy
CO adsorption
CO desorption

ABSTRACT

The influences of support (silica or titania) and loading of Fe promoter on the activity and selectivity of Rh-based catalysts for the direct synthesis of ethanol from syngas were explored. The reaction was performed in a fixed-bed reactor system typically operating at 543 K, 20 atm, WHSV of 8000 $cm^3\,g_{cat}^{-1}\,h^{-1}$ and H_2:CO ratio of 1:1. Characterization by H_2 chemisorption and electron microscopy indicated that rhodium was very highly dispersed on the supports and was in direct contact with the Fe promoter. Although little ethanol was produced over 2 wt% Rh on silica, a similar loading of Rh on titania was active for this reaction. Promotion of 2 wt% Rh/SiO_2 by 1 wt% Fe produced a catalyst that exhibited a 22% selectivity to ethanol, with methane being the primary side-product. Addition of Fe to 2 wt% Rh/titania also improved the selectivity to ethanol with the highest selectivity being 37% for a sample with 5 wt% Fe. The effects of temperature, pressure and H_2:CO ratio on the performance of 2 wt% Rh/TiO_2 and 2 wt% Rh–2.5 wt% Fe/TiO_2 were also studied. Although the influence of pressure and H_2:CO ratio was moderate, higher temperatures clearly increased methane production at the expense of ethanol and methanol. Adsorption and thermal desorption of CO in Ar or H_2 were also studied by DRIFTS spectroscopy on 2 wt% Rh/TiO_2 and 2 wt% Rh–2.5 wt% Fe/TiO_2. The gem-dicarbonyl species that was the primary species on these catalysts at room temperature after exposure to CO was more thermally stable on the Fe-promoted catalyst.

1. Introduction

A promising alternative to petroleum-derived fuels and chemicals is the utilization of coal, natural gas, and biomass to make syngas (CO and H_2) for the production of alcohols and hydrocarbons. Indeed, large-scale facilities for the production of methanol and Fischer–Tropsch hydrocarbons continue to be built around the globe. Although the conversion of syngas to ethanol and higher alcohols is also desirable, highly active and selective catalysts still need to be developed.

Previous studies clearly show that ethanol can be produced from syngas over a wide variety of heterogeneous catalysts including supported Co [1,2], Ni [3], Cu [4–8], Pd [9], and MoS_2 [10–12] and two reviews on the catalysts for the direct synthesis of ethanol from syngas have recently appeared [13,14]. The catalysts for the production of ethanol and other light alcohols from syngas can be classified broadly into 4 categories: (a) Rh-based catalysts, (b) modified high-temperature and low-temperature methanol synthesis catalysts based on ZnO/Cr_2O_3 and $Cu/ZnO/Al_2O_3$, respectively, (c) modified Fischer–Tropsch catalysts based on Co, Fe, and Ru, and (d) modified unsulfided and sulfided Mo-based catalysts. A growing consensus regarding ethanol synthesis from syngas is that supported Rh has a great potential for the reaction [15–21], but suitable supports and promoters are needed to enhance the reactivity of Rh and the current high cost of Rh may hinder its commercial utilization.

One possible reaction scheme for the direct conversion of H_2 and CO to ethanol is shown in Fig. 1 [22]. Although the exact intermediates on the metal surface are subject to debate, Fig. 1 is useful to describe the basic features of the reaction network. Based on this scheme, the four specific functions that a catalyst should perform include:

1. *Dissociation* of the adsorbed CO to form adsorbed carbon (C_a) and oxygen (O_a).
2. *Hydrogenation* of the adsorbed carbon to form an adsorbed methyl species (CH_{3a}).
3. *Insertion* of non-dissociated CO into the methyl species to form an adsorbed acyl species (CH_3CO_a).
4. *Hydrogenation* of the adsorbed acyl species to form the ethanol product.

Rhodium is claimed to be the best catalytic metal for this reaction because of its ability to perform all of these functions [15]. Although large ensembles of Rh^0 atoms adsorb CO dissociatively, single Rh^0 and Rh^+ atoms adsorb CO non-dissociatively and act as CO insertion sites [23].

* Corresponding author. Fax: +1 434 982 2658.
E-mail address: rjd4f@virginia.edu (R.J. Davis).

0021-9517/$ – see front matter
doi:10.1016/j.jcat.2008.10.013

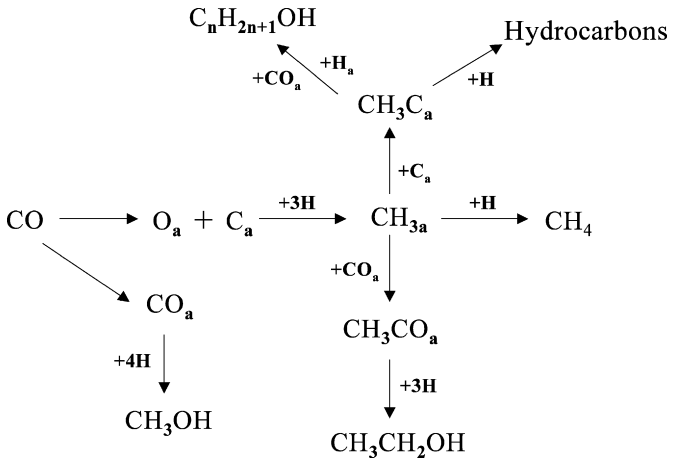

Fig. 1. One possible reaction scheme for direct conversion of H_2 and CO to form ethanol (adapted from [22]).

Burch and Petch showed that Rh particles on a high purity silica support produced very small amounts of ethanol from a glass-lined reactor, with major products being hydrocarbons and a small amount of acetaldehyde [15]. However, addition of Fe to the catalyst significantly improved the product distribution toward ethanol. This study was a warning to the catalysis community since volatile iron carbonyls can deposit onto an Rh catalyst during CO reactions taking place inside a steel reactor. The presence of iron was proposed to stabilize an adsorbed acetyl species (CH_3CHO_a), thus favoring subsequent hydrogenation to ethanol instead of desorption of acetaldehyde [15]. The promotion of Rh is certainly not limited to Fe. In fact, a wide variety of supports as well as promoters can be used to affect the size, nature and the number of active sites for ethanol formation. Although supports such as ceria [18,24], vanadia [19], niobia [25], zirconia [26], and promoters such as V, Nb, Ta [27], Sm [28], and Mo [29] have a positive influence on the reaction, Mn also appears to be a favorable promoter [20,21,30–33]. Examples of other prior art on the catalytic synthesis of hydrocarbons and oxygen-containing compounds from CO and H_2 over supported Rh catalysts include the works of Ichikawa et al. [34,35], Arakawa et al. [36,37], Prins et al. [38,39], and Niemantsverdriet et al. [40,41].

Chuang et al. have summarized the current understanding of ethanol synthesis on supported Rh [23]. The main products from syngas reactions appear to be methane and C_2 oxygenates, which suggests chain growth pathways that form higher hydrocarbons are not important in the reaction network. Oxophilic promoters are claimed to enhance both the CO dissociation step needed to form C atoms on the surface as well as the CO insertion step that accounts for C_2-oxygenates on the surface. More importantly, evidence is provided to support the idea that CO insertion occurs on a single Rh atom and that a positively-charged Rh atom is more active than a neutral one. Thus, a proper balance of CO dissociation, multiple hydrogenation steps, and CO insertion is required to maximize alcohol formation while minimizing methane formation.

The objective of this paper is to clarify the important roles of support (silica or titania) and Fe promoter on the activity of Rh for the direct synthesis of ethanol from syngas. Diffuse reflectance infrared Fourier transform spectroscopy (DRIFTS) was also used to probe the interaction of CO with the Rh catalysts.

2. Experimental methods

2.1. Catalyst synthesis

The supported Rh catalysts were synthesized by incipient wetness impregnation. Granular rhodium nitrate (Pfaltz and Bauer (Waterbury, CT)) was used as the precursor of rhodium for all catalysts.

2.1.1. Synthesis of unpromoted Rh catalysts supported on silica and titania

A 2 wt% Rh/SiO_2 catalyst was prepared by dissolving 0.129 g $Rh(NO_3)_3{\cdot}2H_2O$ in 6 mL of distilled deionized water and adding this solution dropwise with proper kneading to 2 g of silica (Cabot Cab-O-Sil M-5, pre-washed with HNO_3) to the point of incipient wetness. The paste was dried overnight in air at 413 K and subsequently calcined in air at 723 K for 4 h.

Titania-supported Rh catalysts were prepared in a similar manner as described above, except titania (Degussa P-25) was used as the support instead of silica, and the Rh concentration in the solution was adjusted to give the desired loading.

2.1.2. Synthesis of Fe-promoted Rh catalysts supported on silica and titania

As an example, a 2 wt% Rh–1 wt% Fe/TiO_2 catalyst was prepared by dissolving 0.315 g $Rh(NO_3)_3{\cdot}2H_2O$ and 0.36 g $Fe(NO_3)_3{\cdot}9H_2O$ in 7.5 mL of distilled deionized water and adding this solution dropwise with proper kneading to 5 g TiO_2 (Degussa P-25) to the point of incipient wetness. The paste was dried overnight in air at 413 K and subsequently calcined in air at 723 K for 4 h.

Iron-promoted Rh catalysts on silica or titania with various loadings of Fe were prepared in a similar manner with appropriate concentrations of metal precursors.

2.2. Catalyst characterization

The metal loadings of the catalysts were determined by Galbraith Laboratories (Knoxville, TN) using ICP analysis. Additionally, the Rh dispersion was evaluated by H_2 chemisorption performed using a Micromeritics ASAP 2020 automated adsorption system at 308 K. Calcined catalysts were reduced in flowing H_2 at 473 K for 2.5 h and evacuated at that temperature for 2 h prior to cooling in vacuo to 308 K. An H/Rh_{surf} stoichiometry equal to unity was assumed in the analysis.

Electron microscopy was performed on an FEI TITAN field-emission transmission electron microscope equipped with an EDAX Genesis EDS system operated at 200 kV. Catalyst samples in the powdered form were sprinkled onto a copper grid with lacy carbon support film. Images were recorded with a slow scan CCD camera. To analyze individual particles, the electron beam was focused on the middle of the target particle with a diameter slightly lesser than the diameter of the target particle. The EDS spectra were analyzed using FEI TIA software.

2.3. Reactions of CO and H_2

The catalysts were evaluated in a fixed-bed micro-reactor system (Autoclave Engineers' BTRS Jr., Erie, PA). Calcined catalysts were first pressed into pellets, crushed, and size-separated (+40/−80 mesh). Approximately 0.15 g catalyst was intimately mixed with 2.5 g of silicon carbide (Universal Photonics, Inc., Hicksville, NY) and loaded into the reactor. The catalyst was then reduced in flowing dihydrogen (20 $cm^3(STP)\,min^{-1}$) at 573 K for 2 h under atmospheric pressure. Following reduction, the catalysts were tested at nominally identical conditions of 543 K, 20 atm total pressure, syngas (H_2 + CO) flow of 20 $cm^3(STP)\,min^{-1}$, H_2:CO ratio of 1:1, and a WHSV of 8000 $cm^3\,g_{cat}^{-1}\,h^{-1}$. The catalyst bed temperature was monitored by a thermocouple inserted within the catalyst bed. All gases (CO (GT&S) and H_2 (GT&S)) were UHP grade (99.999%). Additionally, CO was purified by passing it through a silica trap immersed in a dewar containing a dry ice–acetone mixture before introduction into the reactor. The results reported here

Table 1
Conversion of syngas over silica- and titania-supported Rh catalysts.

Catalyst	Conversion (%)	%Selectivity								
		CH_4	C_2H_6	C_3H_8	C_4H_{10}	CH_3CHO	CH_3OH	EtOH	PrOH	EthAc
2% Rh/SiO_2	0.75	51.3	19.5	24.2	5.1	0.0	0.0	0.0	0.0	0.0
2% Rh/SiO_2[a] (Burch and Petch [15])	1.52	48.0	5.5	16.0	–	14.0	0.6	0.7	–	2.7
2% Rh–1% Fe/SiO_2	2.70	35.5	9.8	9.1	2.0	2.8	13.5	21.8	3.7	1.9
2% Rh–1% Fe/SiO_2 (Burch and Petch [15])	4.45	38.0	3.1	2.8	–	0.9	11.0	39.0	–	1.2
2% Rh/TiO_2	5.66	47.4	3.2	14.8	5.2	5.7	1.9	11.1	0.0	10.7
2% Rh–1% Fe/TiO_2	7.47	42.4	4.9	10.4	3.4	13.3	1.6	13.4	0.0	10.6

Note. Nominal conditions are $T = 543$ K, $P = 20$ atm, 0.150 g catalyst (40–80 mesh), 2.5 g SiC to dilute the bed, H_2:CO 1:1, syngas flow = 20 cm^3(STP) min^{-1}. Conversion (%) $= \sum n_i M_i \times 100/M_{CO}$ and selectivity $= n_i M_i / \sum n_i M_i$ where n_i is the number of carbon atoms in product i, M_i is the mole percent of product i measured, and M_{CO} is the mole percent of carbon monoxide in the feed.

[a] The balance of selectivity (5.9%) is to acetic acid.

are generally obtained after 2 h on-stream. Two HP 5890 Series II gas chromatographs were integrated downstream of the reactor for the analysis of reactants and products. The first one was equipped with a flame ionization detector and a 50 m-long HP-1 cross-linked methyl silicone gum capillary column to monitor hydrocarbons, alcohols, acetaldehyde, methyl acetate (not observed) and ethyl acetate. The second one was equipped with a thermal conductivity detector and a 6-ft long Alltech CTR packed column and was used to monitor the possible formation of CO_2.

The conversion of CO was based on the fraction of CO that formed carbon-containing products according to:

$$\%\text{Conversion} = \left(\sum n_i \cdot M_i / M_{CO}\right) \cdot 100\%,$$

where n_i is the number of carbon atoms in product i, M_i is the percentage of product i detected, and M_{CO} is the percentage of carbon monoxide in the syngas feed. This equation was valid since differential conversion was maintained throughout this study.

The selectivity to product i is based on the total number of carbon atoms in the product and is therefore defined as:

$$S_i = (n_i \cdot M_i) / \left(\sum n_i \cdot M_i\right).$$

2.4. DRIFTS studies

A Bio-Rad FTIR (FTS-60A) spectrometer outfitted with an MCT detector and a Harrick DRIFTS cell were used for the IR studies. The cell allowed collection of spectra in a controlled environment over a range of temperatures (298–548 K). To obtain the spectra presented here, 100 scans were co-added at resolution of 2 cm^{-1}. The procedure for collection of the DRIFTS spectra was as follows. First, 30–40 mg of powdered catalyst was combined with 70 mg of powdered KBr and the mixture was placed onto the sample holder. The powder surface was carefully flattened to obtain high IR reflectivity. The sample was then heated under flowing Ar (50 $cm^3\,min^{-1}$) to 573 K, reduced in flowing H_2 at 573 K for 2 h, purged in flowing Ar at 573 K, and then cooled to 298 K in flowing Ar. After collecting a background spectrum, CO was admitted to the cell at 50 $cm^3\,min^{-1}$ for approximately 10 min. The gas-phase CO was purged from the cell by flowing Ar and a spectrum of adsorbed CO was collected after purging for 60 min. Thermal desorption experiments (heating rate 10 K min^{-1}) were also performed in either flowing Ar or H_2.

3. Results and discussion

3.1. Influence of support

The first entry in Table 1 illustrates how unpromoted Rh/SiO_2 is a very poor catalyst for syngas conversion. Indeed, only trace amounts of ethanol were produced over this catalyst at our standard conditions. The only products at the conditions of 543 K, 20 atm, H_2:CO 1:1, a syngas flow of 20 $cm^3\,min^{-1}$, and a space velocity of 8000 $cm^3\,g_{cat}^{-1}\,h^{-1}$ were methane and light hydrocarbons. Only trace amounts of ethanol, methanol, acetaldehyde or ethyl acetate were detected over the unpromoted Rh/SiO_2 catalyst. Burch and Petch [15] have also shown that hydrocarbons are generally the preferred reaction products on unpromoted rhodium supported on silica, although acetaldehyde and ethanol can be minor co-products.

Next, a promoted catalyst similar to that used by Burch and Petch (2 wt% Rh–1 wt% Fe/SiO_2) [15] was prepared and tested in our laboratory at conditions similar to those reported by these authors (543 K, 20 atm, 0.150 g catalyst, 2.5 g SiC as the bed diluent, syngas 20 $cm^3\,min^{-1}$, and H_2:CO ratio of 1:1). The results summarized in Table 1 for the Burch and Petch-type catalyst (third entry) compare well to those reported in their paper [15]. The main products were methane, light hydrocarbons (ethane and propane), and light alcohols (methanol and ethanol).

Table 1 also shows a direct comparison of Rh supported on silica to Rh supported on titania. The titania-supported catalyst was not only more active for syngas conversion, but also produced a variety of oxygenate products including methanol, ethanol, acetaldehyde and ethyl acetate. Adding 1 wt% Fe to a 2 wt% Rh/TiO_2 catalyst further improved the CO conversion and oxygenate selectivity. Since both silica and titania alone were inactive for syngas conversion under these conditions, the product formation observed in this study is attributed solely to the transition metal components (Rh/Fe).

The influence of silica and titania support on CO hydrogenation over supported Rh was also investigated in detail by Katzer et al. [42], albeit at different reaction conditions. The conditions used in their work were 473 K, 10 atm, and 4% CO in dihydrogen. Their results also indicate that titania is the more active support for Rh. They reported a 200-fold variation in the product formation rate for titania compared to silica, which was attributed to an increase in the number of active sites for the reaction instead of the changes in the energetics of the reaction.

The effect of iron on the performance of supported rhodium catalysts for CO hydrogenation reactions were also investigated in a pioneering study by Bhasin et al. [43] and later by Guglielminotti et al. [44]. Their results also agree with our findings that iron has a profound effect on the selectivity to ethanol. The first set of authors [43] investigated the performance of Rh and $Rh–Fe/SiO_2$ catalysts using a Berty-type backmixed reactor at nominal conditions of 573 K, 1000 psig, and H_2:CO ratio of 1:1. A nominal loading of 2.5 wt% Rh was used along with five different Fe loadings (0.00 wt%, 0.05 wt%, 0.10 wt%, 0.20 wt%, and 0.50 wt%). Their results show that the performance of a 2.5% Rh–0.20% Fe/SiO_2 catalyst was superior to that of the unpromoted 2.5% Rh/SiO_2 catalyst

in terms of selectivity to ethanol. The selectivity to ethanol for the promoted catalyst was 29.2%, while that for the unpromoted catalyst was only 17%. It also appears that the increase in selectivity to ethanol is at the direct expense of methane selectivity, which reduced to 42.1% for the promoted catalyst from a value of 52.0% for the unpromoted catalyst. Similar results were also reported by Guglielminotti et al. [44] who found that adding Fe to Rh/ZrO_2 increased the selectivity of methanol and ethanol. Their experiments were carried out at 493 K, 1 atm, and a H_2/CO ratio of 3.

Hanaoka et al. [45] examined the effect Rh loading on CO hydrogenation over Rh/SiO_2 catalysts at 553 K, 50 atm, H_2:CO:Ar = 45:45:10, and a flow rate of 100 $cm^3\,min^{-1}$. The Rh loading was varied from 1 wt% to 30 wt%. Although increasing the Rh loading improved the CO conversion, the selectivity to various products was also altered as a function of Rh loading. They found that the selectivity to methane increased monotonically with an increase in Rh loading, at the expense of CH_3OH and C_2H_5OH.

3.2. Role of Rh loading on TiO_2

The effect of Rh loading on the activity and selectivity of titania-supported catalysts is summarized in Table 2. The results show that CO conversion over the catalysts increased with the Rh loading on titania, as expected. The selectivities reported for the low loaded catalyst are somewhat less reliable than the other entries because of very low level of conversion. In general, the selectivities to C_1–C_4 hydrocarbons and to oxygenates were affected little by the Rh loading, in contrast to the results of Hanaoka et al. [45] who reported increasing CH_4 selectivity with increasing Rh loadings.

Table 3 summarizes the results from H_2 chemisorption and elemental analysis. Although the low loaded Rh/TiO_2 catalysts (0.5 wt% and 1 wt%) exhibited 100% dispersion, higher loadings of Rh resulted in lower dispersions. Nevertheless, the calculated turnover frequency that includes both Rh loading and dispersion of Rh on titania was fairly constant at about 0.02 s^{-1} at our standard conditions. The relatively high dispersion of all the catalysts in Table 3 facilitated the promotional role of the support titania on the catalysis by Rh.

Table 2
Effect of Rh loading on syngas conversion over Rh/TiO_2 catalysts.

Catalyst	Conversion (%)	%Selectivity							
		CH_4	C_2H_6	C_3H_8	C_4H_{10}	CH_3CHO	CH_3OH	EtOH	EthAc
0.5% Rh/TiO_2	1.38	60.3	0.0	14.7	5.3	3.7	5.6	10.4	0.0
1% Rh/TiO_2	3.80	50.6	4.1	12.4	3.8	3.5	3.8	12.2	9.7
2% Rh/TiO_2	5.66	47.4	3.2	14.8	5.2	5.7	1.9	11.1	10.7
5% Rh/TiO_2	7.43	42.5	4.1	16.9	6.3	6.8	1.5	10.4	11.5

Notes. Nominal conditions are $T = 543$ K, $P = 20$ atm, 0.150 g catalyst (40–80 mesh), 2.5 g SiC to dilute the bed, H_2:CO 1:1, syngas flow = 20 cm^3(STP)min^{-1}. Conversion (%) = $\sum n_i M_i \times 100/M_{CO}$ and selectivity = $n_i M_i / \sum n_i M_i$ where n_i is the number of carbon atoms in product i, M_i is the mole percent of product i measured, and M_{CO} is the mole percent of carbon monoxide in the feed.

3.3. Influence of Fe loading on $Rh–Fe/TiO_2$

Four different catalysts were prepared and tested to examine the effect of Fe loading and the results are summarized in Table 4.

The first three entries in Table 4 present reactivity results for three separate runs of a 2 wt% Rh–1 wt% Fe/TiO_2 catalyst. The results indicate good experimental reproducibility since the conversion of CO in these three experiments was at 7.47%, 9.02%, and 8.23%.

The well-known suppression of chemisorption achieved by high-temperature reduction of metal particles on titania occurs by the formation of TiO_x overlayers on the active metal and is often termed as strong metal support interaction, or SMSI [46]. Indeed, Logan et al. [47] have directly observed an amorphous titania film that encapsulates titania-supported Rh particles. To investigate the possible effect of TiO_x overlayers on the activity of promoted catalysts, we evaluated the activity and selectivity of 2 wt% Rh–1 wt% Fe/TiO_2 after a high-temperature reduction (HTR) at 748 K and compared the results to those obtained after our standard low-temperature reduction (LTR) at 573 K.

The fourth entry in Table 4 summarizes the results from a catalyst after a high-temperature reduction. The CO conversion and product selectivity are within the experimental error of those associated with the catalyst reduced at low temperature (first three entries of Table 4). Similar conclusions were reported by Katzer et al. [42] who found that although the CO and H_2 chemisorption capacity changes as a function of the reduction temperature, the rate of CO hydrogenation and the product selectivities for Rh/TiO_2 catalysts reduced at 673 K were essentially the same as for Rh/TiO_2 reduced at 473 K. Moreover, Van't Blik et al. [38] also reported that the reduction temperature did not influence to a great extent CO hydrogenation over Rh/Al_2O_3 and Rh/TiO_2. Interestingly, Frydman et al. [25] reported that the rates of CO hydrogenation on monometallic Rh catalysts supported on Nb_2O_5 decreased substantially upon high-temperature reduction, whereas the CO hydrogenation rates for bimetallic catalysts comprised of Co–Rh did

Table 3
Results from elemental analysis and H_2 chemisorption used to determine TOF for Rh/TiO_2 catalysts.

Catalyst composition (nominal)	Rh loading (wt%)	H/Rh (%)	Turnover frequency[a] (s^{-1})
0.5% Rh/TiO_2	0.44%	~100%	0.0149
1% Rh/TiO_2	0.80%	~100%	0.0222
2% Rh/TiO_2	1.60%	88%	0.0206
5% Rh/TiO_2	4.40%	54%	0.0159
2% Rh/SiO_2	Not determined	46%[b]	0.0038

[a] Molecules of CO converted per Rh surface atom per second.
[b] Nominal.

Table 4
Effect of Fe loading on $Rh–Fe/TiO_2$ catalysts for syngas conversion.

Catalyst	Conversion (%)	%Selectivity							
		CH_4	C_2H_6	C_3H_8	C_4H_{10}	CH_3CHO	CH_3OH	EtOH	EthAc
2% Rh–1% Fe/TiO_2	7.47	42.4	4.9	10.4	3.4	13.3	1.6	13.4	10.6
2% Rh–1% Fe/TiO_2	9.02	43.6	3.5	10.8	3.9	13.3	0.0	14.4	10.6
2% Rh–1% Fe/TiO_2	8.23	43.0	3.2	9.7	3.5	13.5	0.0	15.2	11.9
2% Rh–1% Fe/TiO_2 (HTR)	8.65	44.1	2.5	8.0	2.6	13.7	0.0	17.8	11.4
2% Rh–2.5% Fe/TiO_2	9.28	37.9	2.7	4.3	1.1	11.2	2.8	31.0	9.0
2% Rh–5% Fe/TiO_2	6.20	35.3	2.9	3.3	0.8	7.0	4.8	37.2	8.6
2% Rh–10% Fe/TiO_2	5.68	37.3	5.2	4.2	0.9	2.2	14.9	33.2	2.1

Note. Nominal conditions are $T = 543$ K, $P = 20$ atm, 0.150 g catalyst (40–80 mesh), 2.5 g SiC to dilute the bed, H_2:CO 1:1, syngas flow = 20 cm^3(STP)min^{-1}. Conversion (%) = $\sum n_i M_i \times 100/M_{CO}$ and selectivity = $n_i M_i / \sum n_i M_i$ where n_i is the number of carbon atoms in product i, M_i is the mole percent of product i measured, and M_{CO} is the mole percent of carbon monoxide in the feed.

Table 5
Results from elemental analysis and H_2 chemisorption used to determine TOF for Rh–Fe/TiO_2 catalysts.

Catalyst composition (nominal)	Rh and Fe loadings (wt%)	H/Rh (%)	Turnover frequency[a] (s^{-1})
2% Rh–1% Fe/TiO_2	1.81% Rh–0.83% Fe	49%	0.0472
2% Rh–2.5% Fe/TiO_2	2.03% Rh–2.27% Fe	46%	0.0511
2% Rh–5% Fe/TiO_2	1.62% Rh–3.97% Fe	38%	0.0515
2% Rh–10% Fe/TiO_2	1.91% Rh–8.97% Fe	20%	0.0767
2% Rh–1% Fe/SiO_2	Not determined	26%[b]	0.0257

[a] Molecules of CO converted per Rh surface atom per second.
[b] Nominal.

not vary appreciably as a function of reduction temperature. The authors concluded that the combination of the two metals somehow suppressed the negative influence of the high temperature reduction. This phenomenon appears to be a function of the type of catalyst, support, and other physicochemical properties of the catalyst.

The next three entries in Table 4 illustrate the importance of Fe loading on the catalyst. The results show that addition of 2.5 wt% Fe improved the CO conversion while simultaneously increasing the ethanol selectivity from 13.4% to 31.0%. Addition of 5 wt% Fe reduced the conversion of CO, but improved the ethanol selectivity to 37.2%. Addition of 10 wt% Fe continued to reduce the CO conversion on the catalyst, without an additional gain in ethanol selectivity. Increasing the Fe content of the Rh/TiO_2 catalysts also reduced the ethyl acetate and acetaldehyde selectivity. Iron has been claimed to be an effective catalyst for the hydrogenation of acetaldehyde to ethanol in presence of Rh [15].

These results from Fe-promotion are in general agreement with those of Burch and Hayes [17], who studied CO hydrogenation over 2% Rh/γ-Al_2O_3 promoted by Fe (up to 10 wt%) at 543 K, 10 atm, WHSV of 8000 $cm^3\,g_{cat}^{-1}\,h^{-1}$, and H_2:CO ratio of 1:1. Their study, however, revealed a more substantial enhancement of ethanol selectivity (from ca. 2% over an unpromoted Rh/γ-Al_2O_3 to 48% over a Fe-promoted catalyst). Furthermore, the increase in ethanol selectivity was at the expense of methane selectivity, which decreased from ca. 48% over an unpromoted catalyst to about 23% over the Fe-promoted one.

The enhanced selectivity of catalysts toward ethanol formation with an increasing amount of promoter has been attributed to the close interaction between the metal and the promoter, i.e., an increasing interfacial contact between the metal and the promoter [17]. Thus, high loadings of Fe promoter will suppress H_2 chemisorption by a simple covering of the active Rh surface. Table 5 illustrates the observed decrease of exposed Rh with increasing Fe loading on Rh/TiO_2 catalysts. Table 5 also illustrates how Fe promotes the turnover frequency for CO conversion. Evidently, the interfacial sites are substantially more active than the unpromoted Rh/TiO_2 catalysts.

Since the results from H_2 chemisorption and catalytic reaction indicated a substantial interaction between Fe and Rh, we performed electron microscopy on a representative sample. The electron micrograph of 2 wt% Rh–2.5 wt% Fe/TiO_2 in Fig. 2 shows ~2 nm bimetallic particles of Rh and Fe dispersed on titania. The corresponding EDS spectra of the four individual particles marked in Fig. 2 are presented in Fig. 3. In each case, both Rh and Fe are present in the particle.

3.4. Influence of process variables: temperature, pressure, and H_2:CO ratio

The effects of temperature and pressure on the conversion and selectivity of an unpromoted 2 wt% Rh/TiO_2 and promoted 2 wt% Rh–2.5 wt% Fe/TiO_2 are summarized in Tables 6 and 7, respectively.

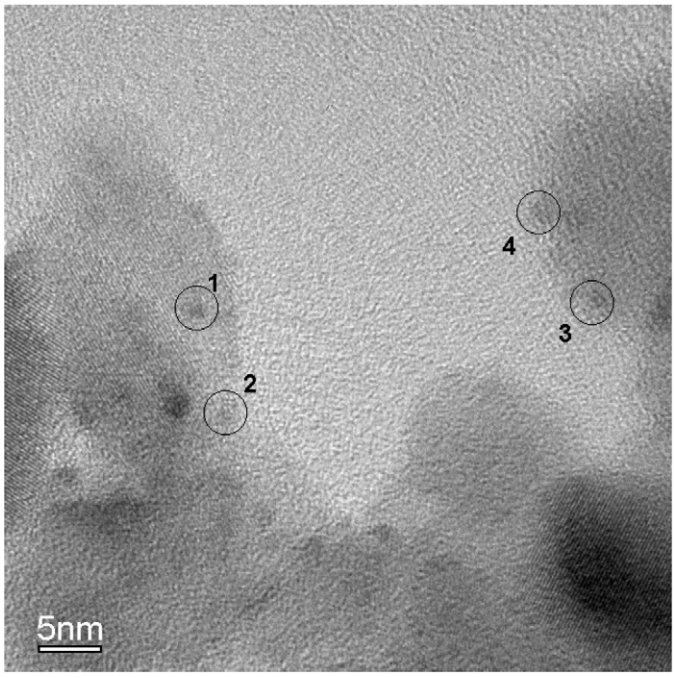

Fig. 2. Electron micrograph of a 2 wt% Rh–2.5 wt% Fe/TiO_2 catalyst.

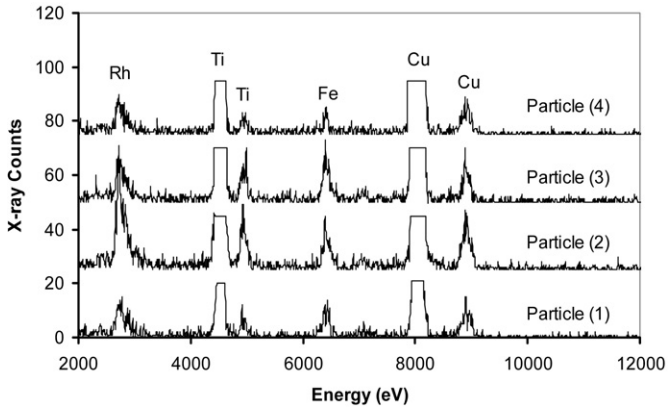

Fig. 3. EDS spectra of particles identified in the electron micrograph in Fig. 2 (spectra are offset for clarity and are truncated for Ti and Cu).

Table 6
Effects of temperature and pressure on the reactions of syngas over a 2 wt% Rh/TiO_2 catalyst.

Condition	1	2	3	4	5
T (K)	503	528	543	543	543
P (atm)	20	20	20	13.6	34
H_2 + CO ($cm^3\,min^{-1}$)	20	20	20	20	20
H_2/CO	1:1	1:1	1:1	1:1	1:1
Conversion (%)	0.83	3.11	5.66	7.08	6.49
Selectivities (%)					
CH_4	36.5	41.8	47.4	48.1	47.9
C_2H_6	0.0	4.1	3.2	4.2	4.2
C_3H_8	11.5	13.6	14.8	15.5	13.0
C_4H_{10}	5.5	4.9	5.2	5.1	3.7
CH_3CHO	5.6	4.5	5.7	4.2	4.4
CH_3OH	10.8	4.4	1.9	2.1	2.2
C_2H_5OH	16.2	13.5	11.1	11.3	11.4
Ethyl acetate	13.9	13.1	10.7	9.3	13.2
CO_2	0.0	0.0	0.0	0.0	0.0

Note. Conversion (%) $= \sum n_i M_i \times 100/M_{CO}$ and selectivity $= n_i M_i / \sum n_i M_i$ where n_i is the number of carbon atoms in product i, M_i is the mole percent of product i measured, and M_{CO} is the mole percent of carbon monoxide in the feed.

Table 7
Effects of temperature and pressure on the reactions of syngas over a 2 wt% Rh–2.5 wt% Fe/TiO_2 catalyst.

Condition	1	2	3	4	5
T (K)	527	543	567	543	543
P (atm)	20	20	20	14	28
H_2 + CO ($cm^3\ min^{-1}$)	20	20	20	20	20
H_2/CO	1:1	1:1	1:1	1:1	1:1
Conversion (%)	4.55	9.3	17.7	6.7	8.8
Selectivities (%)					
CH_4	30.5	37.9	46.7	36.2	37.5
C_2H_6	2.3	2.7	3.8	2.4	2.6
C_3H_8	3.8	4.3	5.8	3.8	4.0
C_4H_{10}	0.5	1.1	0.9	1.0	1.0
CH_3CHO	12.6	11.2	10.9	10.1	11.1
CH_3OH	4.0	2.8	0.0	3.3	2.8
C_2H_5OH	34.6	31.0	23.7	35.7	30.4
Ethyl acetate	11.6	9.0	8.2	7.5	10.6
CO_2	0.0	0.0	0.0	0.0	0.0

Note. Conversion (%) $= \sum n_i M_i \times 100/M_{CO}$ and selectivity $= n_i M_i / \sum n_i M_i$ where n_i is the number of carbon atoms in product i, M_i is the mole percent of product i measured, and M_{CO} is the mole percent of carbon monoxide in the feed.

Table 8
Influence of H_2:CO ratio on the performance of a 2 wt% Rh–1 wt% Fe/TiO_2 catalyst.

Conditions	1	2	3
T (K)	543	543	543
P (atm)	20	20	20
H_2 + CO ($cm^3\ min^{-1}$)	20	20	20
H_2/CO	1:1	2:1	3:1
Conversion (%)	8.23	21.4	33.9
Selectivities (%)			
CH_4	43.0	51.4	58.3
C_2H_6	3.2	4.9	4.7
C_3H_8	9.7	9.5	7.3
C_4H_{10}	3.5	1.6	0.9
CH_3CHO	13.5	7.2	5.4
CH_3OH	0.0	1.9	2.0
C_2H_5OH	15.2	16.2	15.4
Ethyl acetate	11.9	7.3	6.0
CO_2	0.0	0.0	0.0

Note. Conversion (%) $= \sum n_i M_i \times 100/M_{CO}$ and selectivity $= n_i M_i / \sum n_i M_i$ where n_i is the number of carbon atoms in product i, M_i is the mole percent of product i measured, and M_{CO} is the mole percent of carbon monoxide in the feed.

Although the conversion of CO increased with temperature, the selectivity to undesired methane increased at the expense of ethanol and methanol. The influence of pressure on both catalyst activity and selectivity was fairly insignificant compared to the influence of temperature. The results suggest that the hydrogenation of the $(CH_x)_{ad}$ species becomes dominant at high temperature [48] and more generally, the activation energy for the formation of methane appears to be higher than that for ethanol synthesis [48].

The effects of temperature, pressure, and H_2:CO feed ratio on the performance of a 6% Rh–1.5% Mn/SiO_2 catalyst for CO hydrogenation in a microchannel reactor were also investigated by Hu et al. [48]. As expected, the CO conversion increased quite significantly with temperature over the range of 538 K to 573 K. As seen in our study, the selectivity to methane also increased with temperature at the expense of selectivity to ethanol. In general, the mild influence of pressure and the increase in methane production with increasing temperature at the expense of ethanol are consistent with the results for the Fe-promoted Rh/TiO_2 system reported here.

Table 8 summarizes the influence of H_2:CO ratio over the range of 1 to 3 on the conversion and selectivity of syngas conversion reactions over 2 wt% Rh–1 wt% Fe/TiO_2 at 543 K and 20 atm total pressure. Although the CO conversion increased substantially with increasing H_2 in the feed stream, the selectivity to methane also increased at the expense of the oxygenates, namely, acetaldehyde and ethyl acetate.

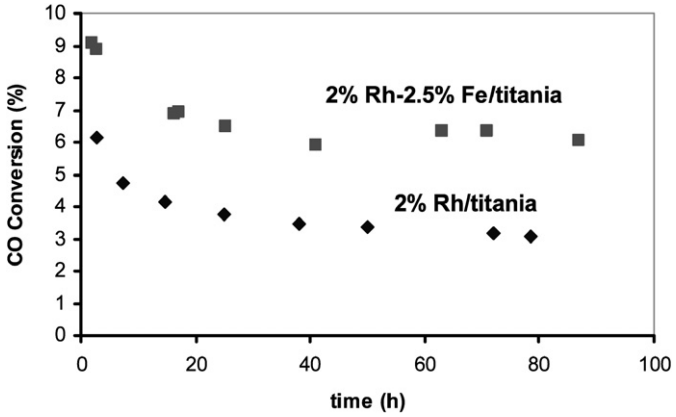

Fig. 4. Deactivation of 2 wt% Rh/TiO_2 and 2 wt% Rh–2.5 wt% Fe/TiO_2 during CO hydrogenation at 543 K and 20 atm.

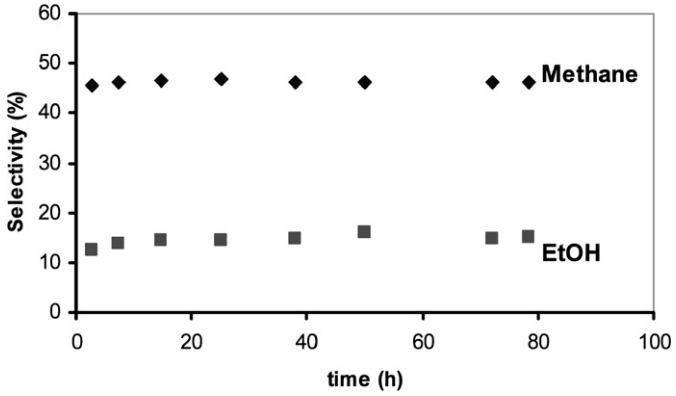

Fig. 5. Selectivity to methane and ethanol over 2 wt% Rh/TiO_2 during the deactivation observed in Fig. 4.

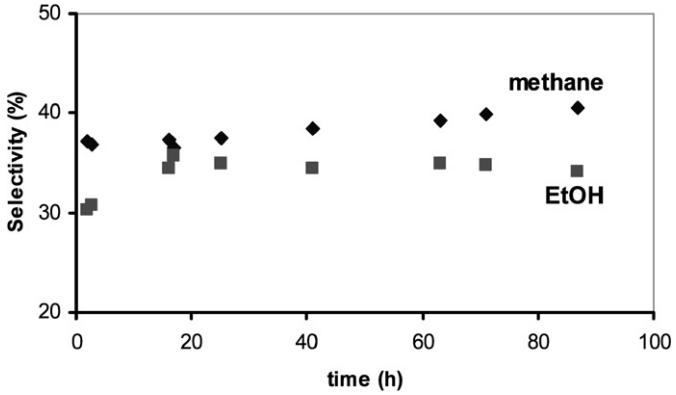

Fig. 6. Selectivity to methane and ethanol over 2 wt% Rh–2.5 wt% Fe/TiO_2 during the deactivation observed in Fig. 4.

It should be noted that CO_2 was never observed as a reaction product. Evidently, the extent of the water–gas shift reaction was negligible under our reaction conditions.

3.5. Stability of unpromoted and Fe-promoted Rh/TiO_2 catalysts

Figs. 4, 5, and 6 illustrate how the CO conversion and product selectivities change with time over an 80-h time interval. For both the unpromoted and promoted Rh/TiO_2, the catalysts deactivated between 30 and 50% of their initial activity over the first

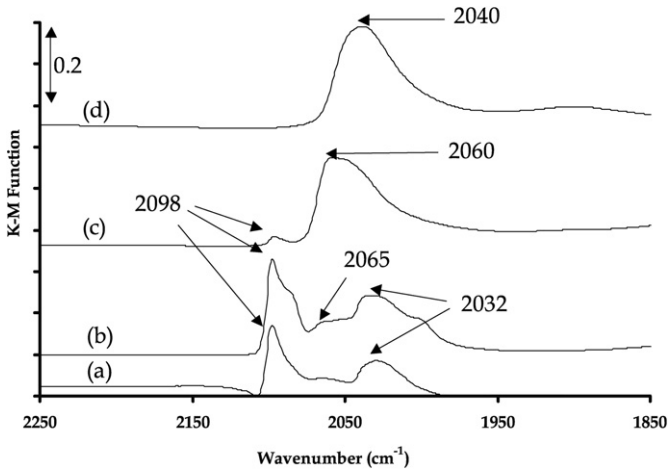

Fig. 7. DRIFTS spectra of adsorbed CO on a 2% Rh/TiO_2: (a) after purging in Ar at room temperature for 60 min, (b) after heating in Ar to 373 K, (c) after heating in Ar to 448 K, (d) after heating in Ar to 548 K.

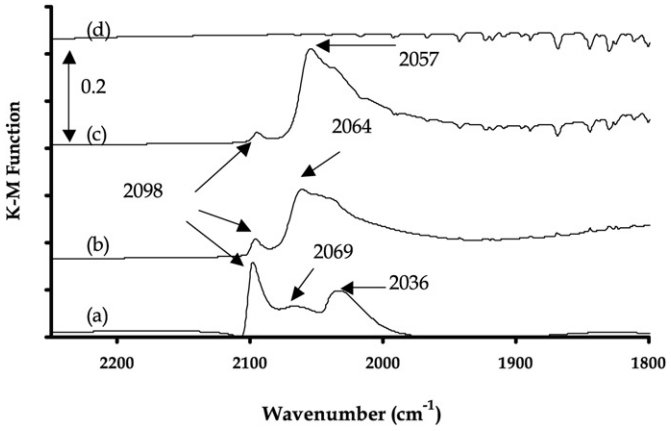

Fig. 8. DRIFTS spectra of adsorbed CO on a 2% Rh/TiO_2: (a) after purging in Ar at room temperature for 60 min, (b) after heating in H_2 to 373 K, (c) after heating in H_2 to 448 K, (d) after heating in H_2 to 548 K.

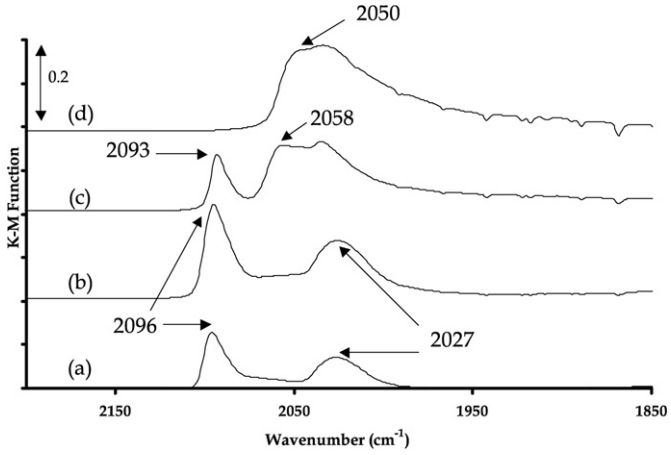

Fig. 9. DRIFTS spectra of adsorbed CO on a 2% Rh–2.5% Fe/TiO_2: (a) after purging in Ar at room temperature for 60 min, (b) after heating in Ar to 373 K, (c) after heating in Ar to 448 K, (d) after heating in Ar to 548 K.

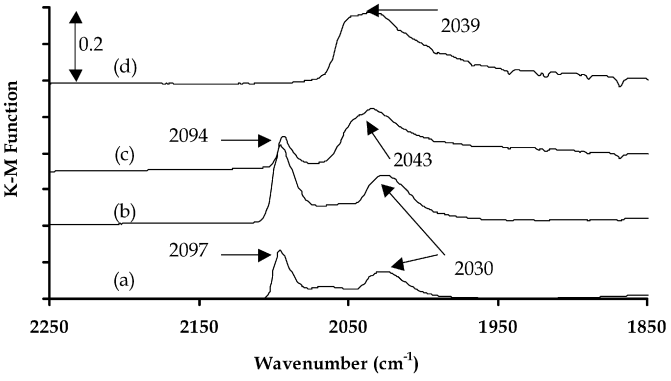

Fig. 10. DRIFTS spectra of adsorbed CO on a 2% Rh–2.5% Fe/TiO_2: (a) after purging in Ar at room temperature for 60 min, (b) after heating in H_2 to 373 K, (c) after heating in H_2 to 448 K, (d) after heating in H_2 to 548 K.

30 h, but were fairly stable thereafter. The selectivity to undesirable methane and desirable ethanol were not significantly affected by deactivation.

3.6. Diffuse reflectance infrared Fourier transform spectroscopy (DRIFTS) studies

In an attempt to relate the structure of the catalyst to its function in CO hydrogenation, we probed the surfaces of an unpromoted and a promoted Rh/TiO_2 catalyst by IR spectroscopy of adsorbed CO. Adsorption of CO on supported Rh at room temperature occurs in three distinct modes, gem-dicarbonyl with characteristic absorption bands at ca. 2100 cm^{-1} and ca. 2030 cm^{-1}, linear CO with absorption band at ca. 2070 cm^{-1}, and bridged CO with a broad absorption band at ca. 1840 cm^{-1}. These assignments were first made in a pioneering work by Yang and Garland [49] and later confirmed by several studies [42,50–54]. In addition to these three modes, additional bands for linear CO on oxidized rhodium (Rh^{2+} at 2135 cm^{-1} and Rh^{3+} at 2145 cm^{-1}), were reported by Trautmann and Baerns [54]. It is now well-accepted that the gem-dicarbonyl species arise from singly-charged Rh^+ species, while linear and bridged CO arise from Rh^0 clusters.

The adsorption of CO at room temperature can lead to an oxidative disruption of Rh^0 clusters into Rh^+ sites. Primet [55] subscribes to the view that CO adsorption on small particles of Rh (<1 nm) is dissociative at room temperature. The chemisorbed oxygen (from CO dissociation) presumably leads to the formation of Rh^+ sites, which then forms the gem-dicarbonyl species upon further adsorption of CO. However, this suggestion was countered by Solymosi and Pasztor [51,56] who found no evidence of CO dissociation on supported Rh particles at temperatures less than 473 K. They proposed instead that the Rh^+ is most probably formed via an oxidation of the Rh^0 clusters by an OH group of the support.

Figs. 7 and 8 show the IR spectra of CO adsorbed on 2 wt% Rh/TiO_2 as a function of temperature in the absence (Fig. 7) and the presence (Fig. 8) of hydrogen. Major spectral changes were observed upon heating in Ar (Fig. 7). The gem dicarbonyl species was stable after heating to 373 K, as illustrated by the strong band at 2098 cm^{-1}. At 448 K, the gem-dicarbonyl band was significantly attenuated while the intensity of the linear CO band at 2060 cm^{-1} increased. At 548 K, the band due to linear CO shifted to 2040 cm^{-1}, which has been seen previously [54]. Although the general behavior of the spectra for desorption of CO in dihydrogen was the same (Fig. 8), there were two major differences. First, the gem-dicarbonyl band was strongly attenuated by heating to only 373 K and second, no features attributable to adsorbed CO were observed at 548 K. The accelerated conversion of the gem-dicarbonyl by dihydrogen agrees with the previous work [53] on a 0.5% Rh/TiO_2.

Figs. 9 and 10 present the IR spectra from similar thermal desorption experiments on 2 wt% Rh–2.5 wt% Fe/TiO_2. Although the spectral features are generally quite similar to the unpromoted sys-

tem, there are some differences that warrant discussion. First, the gem-dicarbonyl species was more stable on the Fe-promoted catalyst since its spectral signature at ca. 2094 cm^{-1} was prominent at 448 K in both Ar (Fig. 9) and H_2 (Fig. 10). Second, the desorption spectrum in presence of dihydrogen (Fig. 10) shows a band at 2039 cm^{-1} due to linear CO at the highest desorption temperature of 548 K. This contrasts the results from a 2% Rh/TiO_2 catalyst where no surface carbonyl was observed at 548 K in H_2 (Fig. 8).

Taken together, these observations suggest that the Fe promoter stabilizes the adsorbed CO on both the charged and neutral Rh moieties.

4. Conclusions

The direct synthesis of ethanol and other oxygenates from CO and H_2 over Rh catalysts depended on the nature of the support and the presence of the Fe promoter. Silica-supported Rh was ineffective at converting CO under the standard conditions used here while titania-supported Rh produced some ethanol and other oxygenates, with methane being the major undesirable hydrocarbon product. Promotion of Rh/silica and Rh/titania with Fe substantially improved the activity of the catalysts and their selectivity to ethanol and other oxygenates. Results from electron microscopy and H_2 chemisorption confirmed the direct interaction of Fe with Rh. Results from thermal desorption of CO from unpromoted and promoted Rh/TiO_2 indicated that Fe stabilized the gem-dicarbonyl formed upon CO adsorption on Rh and retained CO on the Rh at elevated temperatures.

Acknowledgments

The authors acknowledge the seed funding from University of Virginia and partial support from the Chemical Sciences, Geosciences and Biosciences Division, Office of Basic Energy Sciences, Office of Science, U.S. Department of Energy, Grant No. DE-FG02-95ER14549. The authors also acknowledge Dr. Mitsu Murayama for acquisition of electron micrographs and analysis by EDS.

References

[1] X.Q. Qiu, N. Tsubaki, K. Fujimoto, Q.M. Zhu, Fuel Process. Technol. 85 (2004) 1193.
[2] T. Matsuzaki, K. Takeuchi, T. Hanaoka, H. Arawaka, Y. Sugi, Appl. Catal. A 105 (1993) 159.
[3] E.B. Pereira, G.-A. Martin, Appl. Catal. A 103 (1993) 291.
[4] L. Majocchi, L. Lietti, A. Beretta, P. Forzatti, E. Micheli, L. Tagliabue, Appl. Catal. A 166 (1998) 393.
[5] M.J.L. Gines, E. Iglesia, J. Catal. 176 (1998) 155.
[6] M. Xu, E. Iglesia, J. Catal. 188 (1999) 125.
[7] A.B. Stiles, F. Chen, J.B. Harrison, X. Hu, D.A. Storm, H.X. Yang, Ind. Eng. Chem. Res. 30 (1991) 811.
[8] D.J. Elliott, F. Pennella, J. Catal. 114 (1988) 90.
[9] D. He, Y. Ding, H. Luo, C. Li, J. Mol. Catal. A: Chem. 208 (2004) 267.
[10] J. Iranmahboob, H. Toghiani, D.O. Hill, F. Nadim, Fuel Process. Technol. 79 (2002) 71.
[11] J. Iranmahboob, H. Toghiani, D.O. Hill, Appl. Catal. A 247 (2003) 207.
[12] G.-Z. Bian, L. Fan, Y.-L. Fu, K. Fujimoto, Appl. Catal. A 170 (1998) 255.
[13] J.J. Spivey, A. Egbebi, Chem. Soc. Rev. 36 (2007) 1514.
[14] V. Subramani, S.K. Gangwal, Energy Fuels 22 (2008) 814.
[15] R. Burch, M.I. Petch, Appl. Catal. A 88 (1992) 39.
[16] R. Burch, M.I. Petch, Appl. Catal. A 88 (1992) 77.
[17] R. Burch, M.J. Hayes, J. Catal. 165 (1997) 249.
[18] C. Mazzocchia, P. Gronchi, A. Kaddouri, E. Tempesti, L. Zanderighi, A. Kiennemann, J. Mol. Catal. A: Chem. 165 (2001) 219.
[19] P. Gronchi, E. Tempesti, C. Mazzocchia, Appl. Catal. A 120 (1994) 115.
[20] M. Ojeda, M.L. Granados, S. Rojas, P. Terreros, F.J. Garcia-Garcia, J.L.G. Fierro, Appl. Catal. A 261 (2004) 47.
[21] H. Ma, Z. Yuan, Y. Wang, X. Bao, Surf. Interface Anal. 32 (2001) 224.
[22] M. Bowker, Catal. Today 15 (1992) 77.
[23] S.S.C. Chuang, R.W. Stevens Jr., R. Khatri, Top. Catal. 32 (2005) 225.
[24] Y. Wang, J. Li, W. Mi, React. Kinet. Catal. Lett. 76 (2002) 141.
[25] A. Frydman, D.G. Castner, C.T. Campbell, M. Schmal, J. Catal. 188 (1999) 1.
[26] A. Trunschke, H. Ewald, H. Meissner, S. Marengo, S. Martinengo, F. Pinna, L. Zanderighi, J. Mol. Catal. 74 (1992) 365.
[27] T. Beutel, O.S. Alekseev, Y.A. Ryndin, V.A. Likholobov, H. Knozinger, J. Catal. 169 (1997) 132.
[28] H.Y. Luo, W. Zhang, H.W. Zhou, S.Y. Huang, P.Z. Lin, Y.J. Ding, L.W. Lin, Appl. Catal. A 214 (2001) 161.
[29] E. Guglielminotti, E. Giamello, F. Pinna, G. Strukul, S. Martinengo, L. Zanderighi, J. Catal. 146 (1994) 422.
[30] Y. Wang, H. Luo, D. Liang, X. Bao, J. Catal. 196 (2000) 46.
[31] A.S. Lisitsyn, S.A. Stevenson, H. Knozinger, J. Mol. Catal. 63 (1990) 201.
[32] H. Trevino, G.-D. Lei, W.M.H. Sachtler, J. Catal. 154 (1995) 245.
[33] P.-Z. Lin, D.-B. Liang, H.-Y. Luo, C.-H. Xu, H.-W. Zhou, S.-Y. Huang, L.-W. Lin, Appl. Catal. A 131 (1995) 207.
[34] M. Ichikawa, Bull. Chem. Soc. Jpn. 51 (1978) 2273.
[35] A. Fukuoka, T. Kimura, M. Ichikawa, J. Chem. Soc. Chem. Commun. (1988) 428.
[36] H. Arakawa, K. Takeuchi, T. Matsuzaki, Y. Sugi, Chem. Lett. 13 (1984) 1607.
[37] H. Arakawa, T. Fukushima, M. Ichikawa, S. Natsushita, K. Takeuchi, T. Matsuzaki, Y. Sugi, Chem. Lett. 14 (1985) 881.
[38] H.F.J. Van't Blik, J.C. Vis, T. Huizinga, R. Prins, Appl. Catal. 19 (1985) 405.
[39] B.J. Kip, F.W.A. Dirne, J. van Grondelle, R. Prins, Appl. Catal. 25 (1986) 43.
[40] D.C. Koningsberger, C.P.J.H. Borgmans, A.M.J. van Elderen, B.J. Kip, J.W. Niemantsverdriet, J. Chem. Soc. Chem. Commun. (1987) 892.
[41] J.W. Niemantsverdriet, S.P.A. Louwers, J. van Grondelle, A.M. van der Kraan, F.W.H. Kampers, D.C. Koningsberger, in: Proc. 9th Int. Congr. Catal., Calgary, Alberta, vol. 2, 1988, p. 674.
[42] J.R. Katzer, A.W. Sleight, P. Gajardo, J.B. Michel, E.F. Gleason, S. McMillan, Faraday Discuss. Chem. Soc. 72 (1981) 121.
[43] M.M. Bhasin, W.J. Bartley, P.C. Ellgen, T.P. Wilson, J. Catal. 54 (1978) 120.
[44] E. Guglielminotti, F. Pinna, M. Rigoni, G. Strukul, L. Zanderighi, J. Mol. Catal. A 103 (1995) 105.
[45] T. Hanaoka, H. Arakawa, T. Matsuzaki, Y. Sugi, K. Kanno, Y. Abe, Catal. Today 58 (2000) 271.
[46] S.J. Tauster, S.C. Fung, R.L. Garten, J. Am. Chem. Soc. 100 (1978) 170.
[47] A.D. Logan, E.J. Braunschweig, A.K. Datye, D.J. Smith, Langmuir 4 (1988) 827.
[48] J. Hu, Y. Wang, C. Cao, D.C. Elliott, D.J. Stevens, J.F. White, Catal. Today 120 (2007) 90.
[49] A.C. Yang, C.W. Garland, J. Phys. Chem. 61 (1957) 1504.
[50] J.T. Yates, T.M. Duncan, S.D. Worley, R.W. Vaughan, J. Chem. Phys. 70 (1979) 1219.
[51] F. Solymosi, M. Pasztor, J. Phys. Chem. 89 (1985) 4789.
[52] P. Gibson, P.C. van Berge, S. Afr. J. Chem. 44 (1991) 1.
[53] Z.L. Zhang, A. Kladi, X.E. Verykios, J. Mol. Catal. 89 (1994) 229.
[54] S. Trautmann, M. Baerns, J. Catal. 150 (1994) 335.
[55] M. Primet, J. Chem. Soc. Faraday Trans. 1 74 (1978) 2570.
[56] F. Solymosi, M. Pasztor, J. Phys. Chem. 90 (1986) 5312.